

Rotating MHD Heat and Mass Transfer Flow of Nanofluid past Exponentially Stretching Sheet with Second Order Slip

M. Nagasasikala ^a B. Lavanya ^{b*} Jyothikiran. S ^c

^a Lecturer in Mathematics Government Degree College (A) Anantapuramu – 515003, A.P., India

^{b*} Department of Mathematics Associate Professor Manipal Institute of Technology MAHE,
Manipal-576104, KA, India

^c Assistant Professor in Mathematics Govrenment First grade college Tiptur -572201 , Tumkur
District KA, India

^{b*}Email: lavanya.b@manipal.edu

Abstract

In the current paper we research the consolidated impact of Corridor flows, turn, compound response and dissemination on non-Darcy convective warmth and mass exchange stream of nanofluids through a permeable medium past an exponentially extending sheet. By utilizing Runge Kutta shooting technique the overseeing conditions have been assessed for various varieties. It is discovered that the direct and rotational speeds, nanoparticle volume part improve with Corridor pall boundary and diminishes with pivot boundary while the temperature lessens with m and increments with R .

Keywords: Second order slip; Hall currents; Rotation; Chemical reaction; Dissipation; Nanofluid;

1. Introduction

Nanofluids are nanoscale colloidal suspensions containing thick nanomaterials. They are two-stage systems with one phase (solid stage) in another (liquid stage). Nanofluids are conceivable warm energy move fluids with raised thermo actual properties and warmth move execution can be started in numerous gadgets for better requirement (for example energy, heat move and different exhibitions). In nanotechnology, a molecule is characterized as little substances that respond as an ideal unit with respect to its vehicle and assets Nanofluids have been found to have improved thermophysical properties, for example, warm conductivity, warm diffusivity, consistency, and convective warmth move coefficients contrasted with those of base liquids like oil or water. It has shown incredible expected applications in numerous fields. For a two-stage framework, there are some significant issues we need to confront. One of the main issues is the strength of nanofluids, and it stays a major test to accomplish wanted solidness of nanofluids. In this paper, we will survey the new advancement in the strategies for getting ready stable nanofluids and sum up the solidness systems. The enthusiasm for this wonder is because of its potential for use in designing, liquid metal cleaning, staple and synthetic ventures, pressure and infusion forming, and so forth Pressing Nanofluid stream pictures brag cast of utilizations at the business level, for example, oil, biochemical innovation, staple designing and medication make.

Navier [1823] presented a limit condition which expresses that the digressive segment of liquid speed is corresponding to unrelated pressure. Afterward, a few specialists [Shikhmurzear [1993], Choi et al. [2002], and Matthews [2007]] expanded the Navier limit conditions. Various examinations [Martin [2000, 2006], Ariel [2007], Wang [2009]] have been done systematically and mathematically with respect to the slip stream systems over surfaces. These outcomes exhibited that the limit layer condition can be utilized to examine stream at the

Rotating MHD Heat and Mass Transfer Flow of Nanofluid past Exponentially Stretching Sheet with Second Order Slip

miniature electro mechanical framework (MEMS) scale. Das [2012] investigated the convective warmth move normal for Nanofluid over a porous extending surface with fractional slip speed.

Sarojamma et al [2015, 2015] have examined the impact of Corridor Impact, scattering and Warmth sources on convective warmth and mass exchange stream of a Nanofluid past a permeable extending surface. Bhim Sen Kala et al. [2015] examined the joined impact of attractive, penetrability and Forchheimer boundaries on consistent progression of a nanofluids past a permeable extending surface. Limit layer move through dramatically extending sheet within the sight of separated medium by utilizing Shooting technique was considered Swathy Mukopadhyay [2013], Pavitra and Giresha [2013] utilized Runge-Kutta strategy and dissected radiation impact on dusty liquid over a dramatically extending sheet, Zaimi et al. [2014] investigated consistent two dimensional progression of a Nanofluid over an extending/contracting sheet .Wang and Muzumdar [2007] have given great writing on heat move attributes of nanofluids. Sugunamma et al. [2015] have talked about MHD limit layer stream past an extending sheet with reality subordinate inward warmth source. Rushi Kumar [2014] has talked about MHD limit layer stream on warmth and mass exchange over an extending sheet and slip impacts. Sandeep et al. [2015] have examined precarious MHD radiative stream and warmth move of a dusty Nanofluid over a dramatically extending surface Nanofluid through a permeable medium past a dramatically extending surface.

The examination of alluring field sway on fluid stream has huge applications in material science and planning. Mabood and Khan [2014] discussed Magneto-hydrodynamic (MHD) stagnation point stream in porous medium. Kalidas et al. [2017] has separated Cuo-water Nanofluid stream incited by a vertical expanding sheet in presence of an alluring field with convective warmth move.

In this paper, we discover the impact of second sales slip on hydro engaging turning non-Darcy convective warmth and mass exchange stream of a Nanofluid through a vulnerable medium past a permeable drastically widening surface with predictable warmth and mass change inside observing warmth source. The non-quick, coupled controlling conditions have been loosened up by fourth sales Runge-Kutta–shooting philosophy. The speed, rotational speed, temperature and nanoparticle volume segment have been reviewed graphically for various varieties of managing limits. The skin contact, development of warmth and mass exchange on the divider has been assessed mathematically for various groupings.

1.1 Structure

We consider as far as possible layer stream with rotational (dashing) development over an expanding surface in a porous medium stacked up with nanofluids. A uniform alluring field is applied conventional to the plate. Expecting the alluring Reynolds number to be little we ignore the started appealing field. The liquid is accepted to be electrically driving, the convecting liquid and the permeable medium are any spot in thermodynamic harmony. It is recognized that the uniform temperature of the surface is T_w and that of the nanofluids volume division is C_w , the uniform temperature and nanofluids volume segment in the enveloping (free stream district) liquid are (free stream region) fluid are T_∞ and C_∞ independently . There is no rotational improvement of the incorporating (free stream area) fluid.

It is likewise expected that the plate is dramatically stressed with a speed , $u_w(x) = c \exp(\frac{x}{L})$ where c is a positive steady and having no concealed rotational development. The stream should be high so an advective term and a Forchheimer quadratic drag term do show up in the energy conditions. The slushy dispersal and radiation terms have not been estimated.

The schematic chart Fig.1.

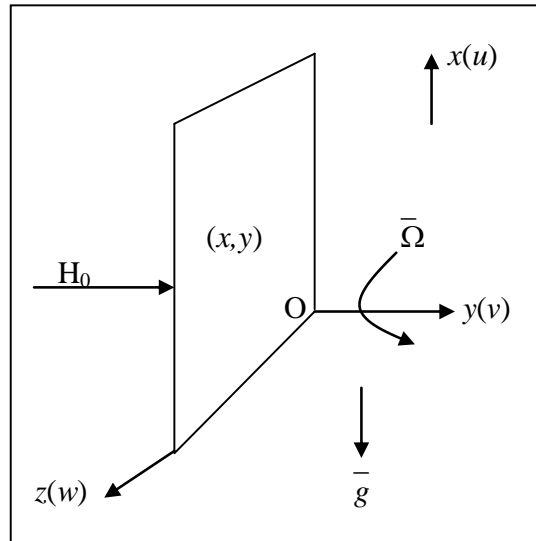


Fig. 1 : Configuration of the Problem

Under these questions, the going with five field conditions exemplifying the confirmation of complete mass, energy (Brinkman-Forchheimer conditions), energy and nanofluids volume partition conditions for the nanofluids are considered as follows:

(i) Equation of continuity:

$$\frac{\partial u}{\partial x} + \frac{\partial v}{\partial y} = 0 \tag{1}$$

(ii) Momentum equations:

$$u \frac{\partial u}{\partial x} + v \frac{\partial u}{\partial y} = \left(\frac{\mu}{\rho_f}\right) \frac{\partial^2 u}{\partial y^2} - \frac{\sigma \mu_e^2 H_o^2}{\rho_f} (u + mw) - \left(\frac{\mu}{k}\right) u - \left(\frac{b}{k}\right) u^2 + 2\Omega w - (\beta \rho_{f\infty}) g (1 - C_\infty) (T - T_\infty) - (\rho_p - \rho_{f\infty}) g (C - C_\infty) \tag{2}$$

$$u \frac{\partial w}{\partial x} + v \frac{\partial w}{\partial y} = \left(\frac{\mu}{\rho_f}\right) \frac{\partial^2 w}{\partial y^2} + \frac{\sigma \mu_e^2 B^2}{\rho_f} (mu - w) - \left(\frac{\mu}{k}\right) w - \frac{b}{\sqrt{k}} w^2 - 2\Omega u \tag{3}$$

(iii) Equation of Energy:

$$u \frac{\partial T}{\partial x} + v \frac{\partial T}{\partial y} = k_f \frac{\partial^2 T}{\partial y^2} - \frac{Q_H}{\rho C_p} (T - T_\infty) + \frac{v}{C_p} \left(\left(\frac{\partial u}{\partial y}\right)^2 + \left(\frac{\partial w}{\partial y}\right)^2 \right) + \frac{\sigma B_o^2}{\rho(1+m^2)} (u^2 + w^2) + \frac{(\rho C)_p}{(\rho C)_f} \left(D_B \frac{\partial T}{\partial y} \frac{\partial C}{\partial y} + \frac{D_T}{T_\infty} \left(\frac{\partial T}{\partial y}\right)^2 \right) \tag{4}$$

(iv) Equation of Mass:

$$u \frac{\partial C}{\partial x} + v \frac{\partial C}{\partial y} = D_B \frac{\partial^2 C}{\partial y^2} + \frac{D_T}{T_\infty} \left(\frac{\partial^2 T}{\partial y^2}\right) - kc(C - C_\infty) \tag{5}$$

where x and y are Cartesian directions along the extending divider and typical to it separately. u and v are the speed segments along the x-pivot and y-hub and w being rotational speed about typical to x-y plane for example about z-hub. T is the temperature in the liquid stage. C is the nanoparticle dimension portion

$B(x) = B_0 \exp\left(\frac{x}{L}\right)$ is flexible magnetic field and B_0 is constant,

Rotating MHD Heat and Mass Transfer Flow of Nanofluid past Exponentially Stretching Sheet with Second Order Slip

$T_w = T_\infty + A \text{Exp}(\frac{x}{2L}), C_w = C_\infty + B \text{Exp}(\frac{x}{2L})$ are the wall temperature and concentration respectively

and A, B are constants, k is the permeability of the porous medium, b is Forchheimer coefficient, Ω is coefficient of rotational motion. ρ, ν and μ are the density, Kinematic viscosity and dynamic viscosity of the fluid, individually. Further, $(\rho C_p)_f$ is the heat capacity of the fluid, $(\rho C_p)_p$ is the effective heat capacity of the nanoparticle solid and k_f is the effective thermal conductivity of the porous medium. The coefficient that shows up in (2.4) and (2.5) are the source coefficient Q_H the Brownian dispersion coefficient D_B and the Thermophoresis dissemination coefficient D_T .

The limit conditions pertinent to the issue are

$$\begin{aligned}
 y = 0 : u &= u_w(x) + A'_{11} \frac{\partial u}{\partial y} + A'_{22} \frac{\partial^2 u}{\partial y^2} = c \text{Exp}(\frac{x}{L}) + A'_{11} \frac{\partial u}{\partial y} + A'_{22} \frac{\partial^2 u}{\partial y^2}, \\
 v &= v_w, w(x, 0) = 0, -k_f \frac{\partial T}{\partial y} = q_w \text{Exp}(\frac{x}{2L}), -D_B \frac{\partial C}{\partial y} = m_w \text{Exp}(\frac{x}{L}) \\
 y \rightarrow \infty : u &\rightarrow 0, w(x, y) \rightarrow 0, T \rightarrow T_\infty, C \rightarrow C_\infty; \\
 \text{where } v_w(x) &= c \text{Exp}(\frac{x}{2L})
 \end{aligned} \tag{6}$$

Introducing the non-dimensional variables as

$$\left. \begin{aligned}
 \eta &= \left(\frac{c}{2\nu L} \right) \exp(\frac{x}{2L}), \psi = (\sqrt{2c\nu L}) \text{Exp}(\frac{x}{2L}) f(\eta), \theta(\eta) = \frac{(T - T_\infty)}{(q_w / k_f)(2\nu L / c)}, \\
 \phi(\eta) &= \frac{C - C_\infty}{(m_w / c)(2\nu L)}, u = \frac{\partial \psi}{\partial y}, v = -\frac{\partial \psi}{\partial x}, w(x, y) = c \text{Exp}(\frac{x}{L}) g(\eta)
 \end{aligned} \right\} \tag{7}$$

Here η is similarity variable, ψ is the stream function, θ is non-dimensional temperature, ϕ is the non-dimensional nanoparticle capacity fraction.

Expanding equation (7), the governing equations (2-5) reduces to

$$\begin{aligned}
 f''' + ff'' - 2(f')^2 - \frac{M^2}{1+m^2}(f' + mg_o), -D^{-1}g_o + fs(f')^2 + \\
 + Rg_o + G(\theta - N\phi) = 0
 \end{aligned} \tag{8}$$

$$g_o + fg_o - 2f'g_o - R1f' + \frac{M^2}{1+m^2}(mf' - g_o) - D^{-1}g_o + Fs(g_o)^2 = 0 \tag{9}$$

$$\begin{aligned}
 \theta'' + \text{Pr}(f\theta' - f'\theta) - Q\theta + Nb\theta'\phi' + Nt(\theta')^2 + \text{Pr}Ec((f'')^2 + (g_o)^2) + \\
 + \frac{\text{Pr}EcM^2}{1+m^2}(f'^2 + g_o^2) = 0
 \end{aligned} \tag{10}$$

$$\phi'' + Le(f\phi' - f'\phi) + \left(\frac{Nt}{Nb}\right)\theta'' - (Le\gamma)\phi = 0 \tag{11}$$

and the boundary conditions the equation (6) are

$$f(0) = fw, f''(0) = 1 + A_{11}f''(0) + A_{22}f'''(0), \theta'(0) = -1, \phi'(0) = -1$$

$$f'(\eta) \rightarrow 0, \theta(\eta) \rightarrow 0, \phi(\eta) \rightarrow 0 \text{ as } \eta \rightarrow \infty \tag{12}$$

where $fw = -v_0 / \left(\frac{c\nu}{2L}\right)$ is the wall mass transfer parameter

$fw > 0$ ($v_0 < 0$) looks like to mass attractions and $fw < 0$ ($v_0 > 0$) consents to mass infusion. he boundaries happening in the conditions (8) - (11) are exhibited as follows

$$M = \frac{2\sigma B_o^2 L}{\rho_f c} e^{-\frac{x}{L}}, D^{-1} = \frac{kce^{\frac{x}{L}}}{2Lv}, Fs = \frac{2bL}{\sqrt{k}}, Pr = \frac{\mu C_p}{k_f}, \nu = \frac{\mu}{\rho}$$

$$Le = \frac{\nu}{D_B}, Nb = D_B \frac{(\rho C)_p (C_w - C_\infty)}{(\rho C)_f}, Nt = \frac{D_T}{T_\infty} \frac{(\rho C)_p (T_w - T_\infty)}{(\rho C)_f},$$

$$Q = \frac{Q_H (c/2L)}{e^{-\frac{x}{L}}}, R1 = \frac{4\Omega L}{U}, \gamma = \frac{k_c (c/2L)}{e^{-\frac{x}{L}}}, U = ce^{\frac{x}{L}}$$

$$A_{11} = \frac{cA'_{11} \text{Exp}\left(\frac{x}{2L}\right)}{2\nu L}, A_{22} = \frac{c^2 A'_{22} \text{Exp}\left(\frac{x}{L}\right)}{(2\nu L)^2}, G = \frac{(\rho\beta)_f gT_o \text{Exp}(-x/2L)}{\mu c}, N = \frac{(\rho_f - \rho_{f\infty})(C_w - C_\infty)}{(\beta)(T_w - T_\infty)}$$

$Q_H = Q (c/2L)e^{\frac{x}{L}}$ is the non-uniform warmth age/assimilation coefficient where $Q > 0$ and $Q < 0$ represent heat producing and ingestion boundaries correspondingly. R1 is the liquid rotational boundary, A11 is the principal request slip boundary, A22 is the subsequent request slip boundary, $U = ce^{\frac{x}{L}}$ is the liquid speed contingent dramatically on x.

The quantities of actual notification for this issue are the neighbourhood skin erosion because of straight movement (Cf), nearby skin grinding because of revolution (Cg), neighbourhood Nusselt number (Nu), neighborhood Sherwood number (Sh). These are characterized as follows

$$C_f = \frac{\tau_w}{0.5\rho U_w^2} = \frac{\mu\left(\frac{\partial u}{\partial y}\right)_{y=0}}{0.5\rho U_w^2} \Rightarrow C_f = \frac{1}{\sqrt{2R_{ex}}} f'(0), \quad C_g = -\frac{1}{\sqrt{2R_{ex}}} g(0), R_{ex} = u_w x / \nu$$

$$Nux = 1/\theta(0) \quad Shx = 1/\phi(0)$$

Rotating MHD Heat and Mass Transfer Flow of Nanofluid past Exponentially Stretching Sheet with Second Order Slip

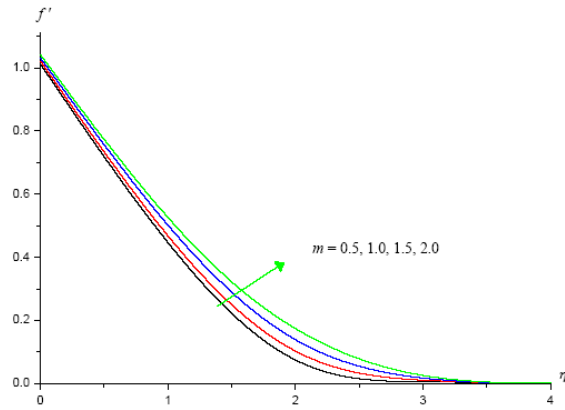


Fig.2a Variation of axial velocity(f') with m
 $R=0.5, Rd=0.5, Ec=0.01, fs=0.2, A11=0.2, A22=-0.02$

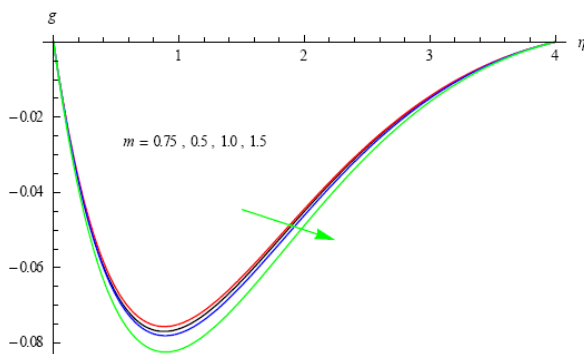


Fig.2b Variation of secondary velocity(g)with m
 $R=0.5, Rd=0.5, Ec=0.01, fs=0.2, A11=0.2, A22=-0.02$

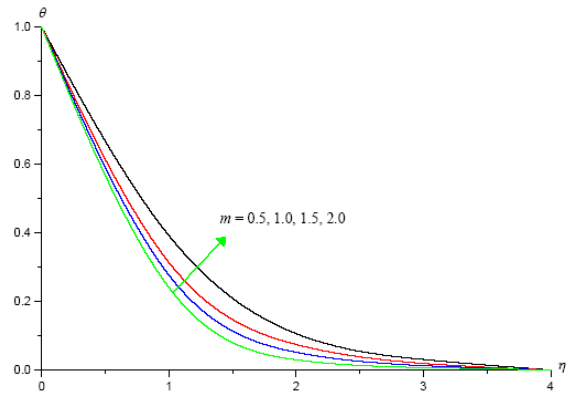


Fig.2c Variation of temperature(θ) with m
 $R=0.5, Rd=0.5, Ec=0.01, fs=0.2, A11=0.2, A22=-0.02$

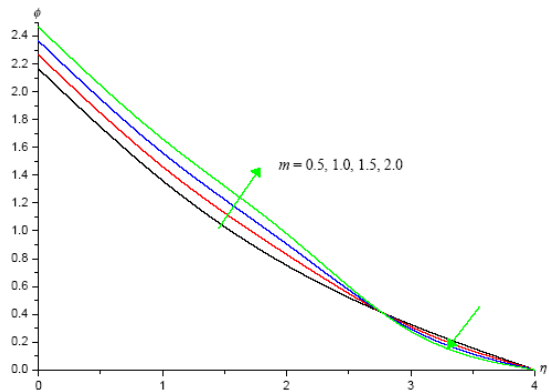


Fig.2d Variation of nanoconcentration(ϕ) with m
 $R=0.5, Rd=0.5, Ec=0.01, fs=0.2, A11=0.2, A22=-0.02$

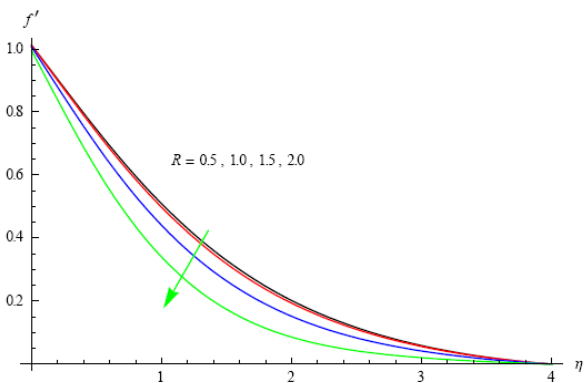


Fig.3a Variation of axial velocity(f') with R
 $m=0.5, Rd=0.5, Ec=0.01, fs=0.2, A11=0.2, A22=-0.02$

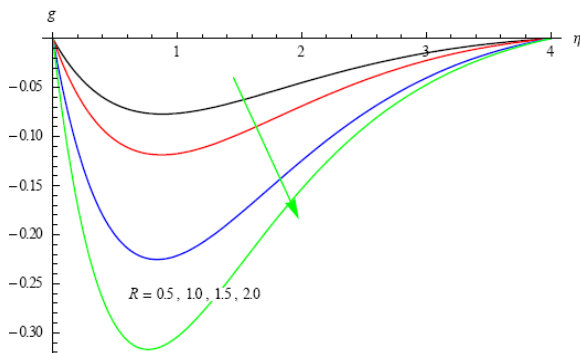


Fig.3b Variation of secondary velocity(g)with R
 $m=0.5, Rd=0.5, Ec=0.01, fs=0.2, A11=0.2, A22=-0.02$

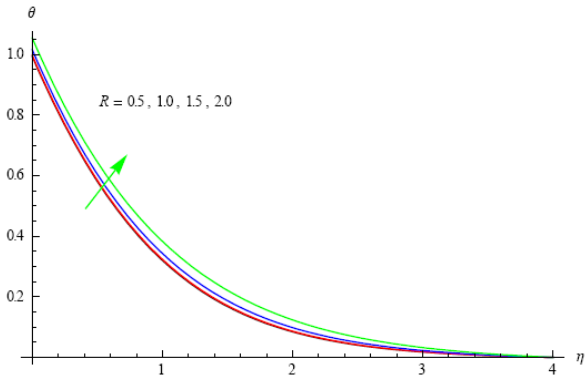


Fig.3c Variation of temperature(θ) with R
 $m=0.5, Rd=0.5, Ec=0.01, fs=0.2, A11=0.2, A22=-0.02$

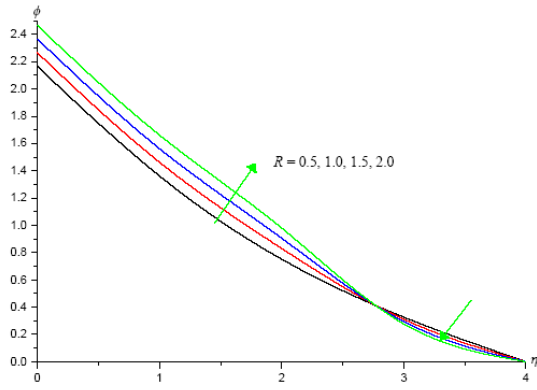


Fig. 3d Variation of nanoconcentration(ϕ) with R
 $m=0.5, Rd=0.5, Ec=0.01, fs=0.2, A11=0.2, A22=-0.02$

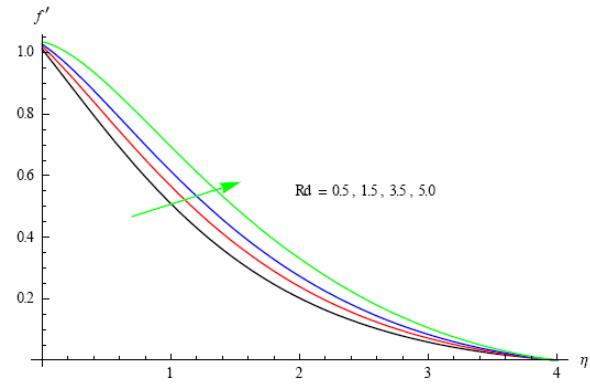


Fig. 4a Variation of axial velocity(f') with Rd
 $m=0.5, R=0.5, Ec=0.01, fs=0.2, A11=0.2, A22=-0.02$

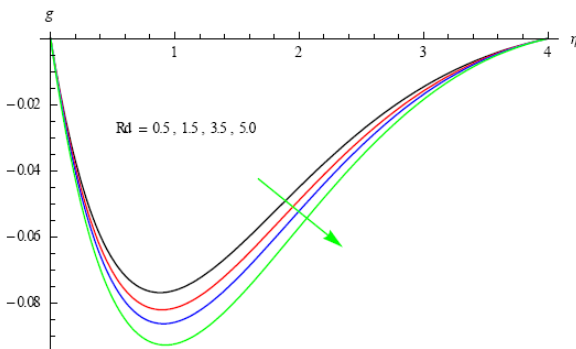


Fig. 4b Variation of secondary velocity(g) with Rd
 $m=0.5, R=0.5, Ec=0.01, fs=0.2, A11=0.2, A22=-0.02$

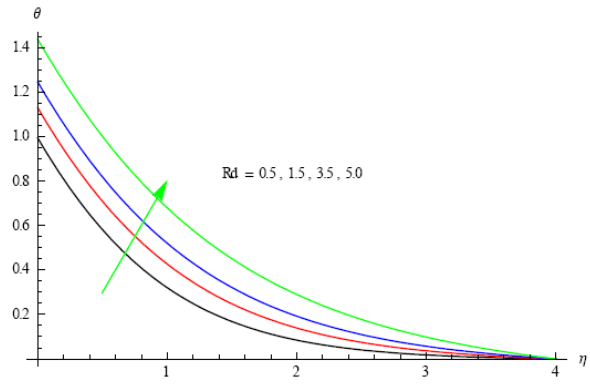


Fig. 4c Variation of temperature(θ) with Rd
 $m=0.5, R=0.5, Ec=0.01, fs=0.2, A11=0.2, A22=-0.02$

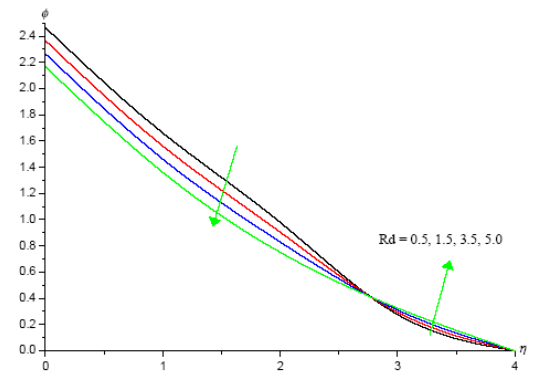


Fig. 4d Variation of nanoconcentration(ϕ) with Rd
 $m=0.5, R=0.5, Ec=0.01, fs=0.2, A11=0.2, A22=-0.02$

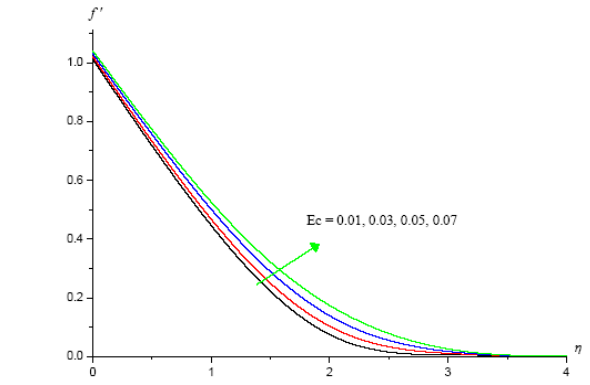


Fig. 5a Variation of axial velocity(f') with Ec
 $m=0.5, R=0.5, Rd=0.5, fs=0.2, A11=0.2, A22=-0.02$

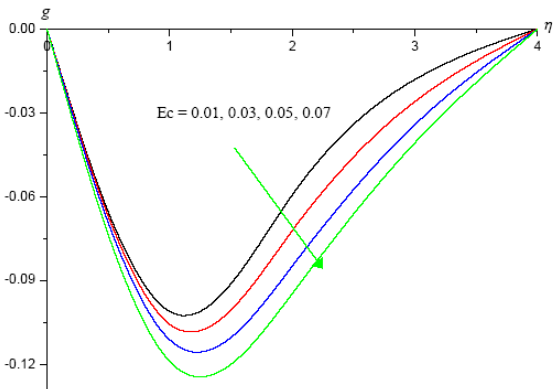


Fig. 5b Variation of secondary velocity(g) with Ec
 $m=0.5, R=0.5, Rd=0.5, fs=0.2, A11=0.2, A22=-0.02$

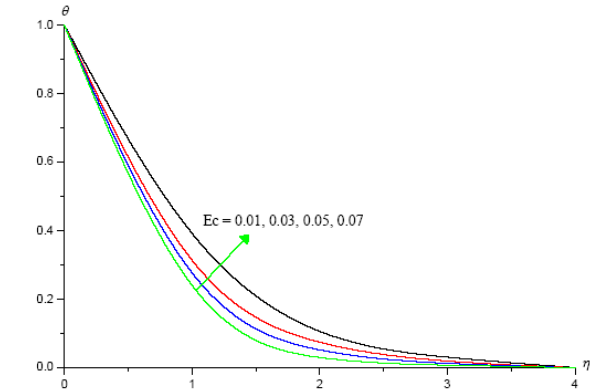


Fig. 5c Variation of temperature(θ) with Ec
 $m=0.5, R=0.5, Rd=0.5, fs=0.2, A11=0.2, A22=-0.02$

Rotating MHD Heat and Mass Transfer Flow of Nanofluid past Exponentially Stretching Sheet with Second Order Slip

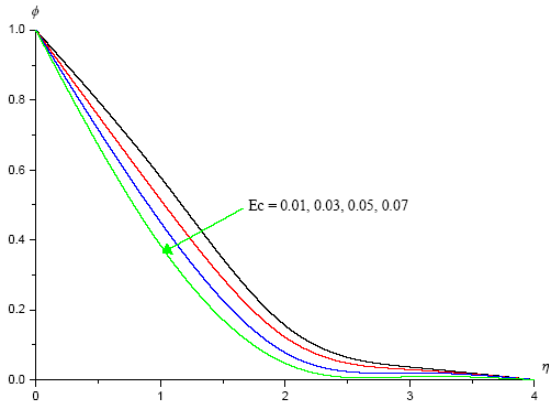


Fig.5d Variation of nanoconcentration(ϕ) with Ec
 $m=0.5, R=0.5, Rd=0.5, fs=0.2, A11=0.2, A22=-0.02$

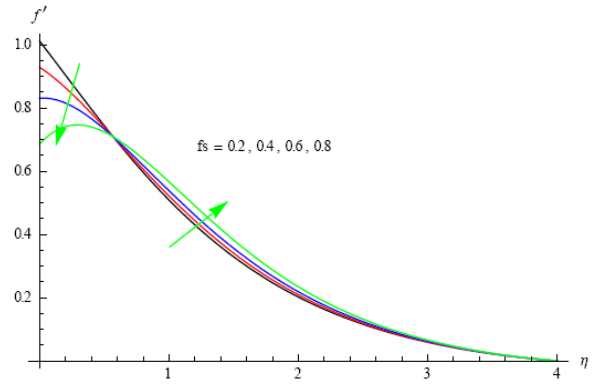


Fig.6a Variation of axial velocity(f') with fs
 $m=0.5, R=0.5, Rd=0.5, Ec=0.01, A11=0.2, A22=-0.02$

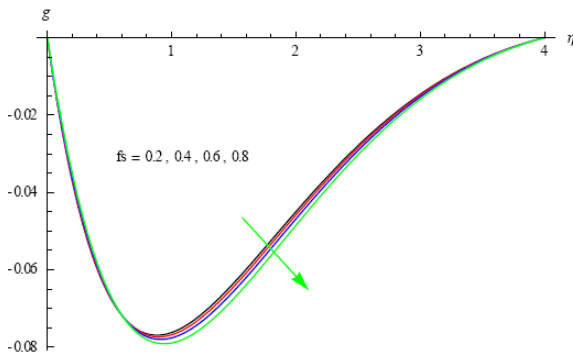


Fig.6b Variation of secondary velocity(g)with fs
 $m=0.5, R=0.5, Rd=0.5, Ec=0.01, A11=0.2, A22=-0.02$

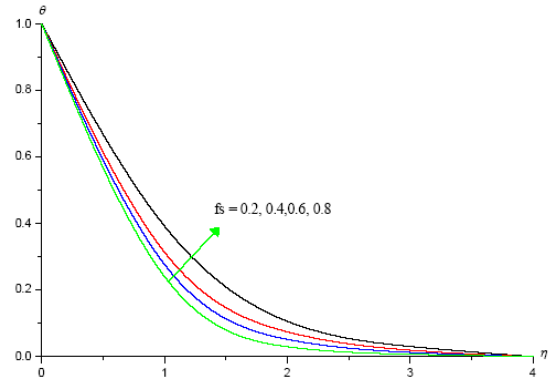


Fig.6c Variation of temperature(θ) with fs
 $m=0.5, R=0.5, Rd=0.5, Ec=0.01, A11=0.2, A22=-0.02$

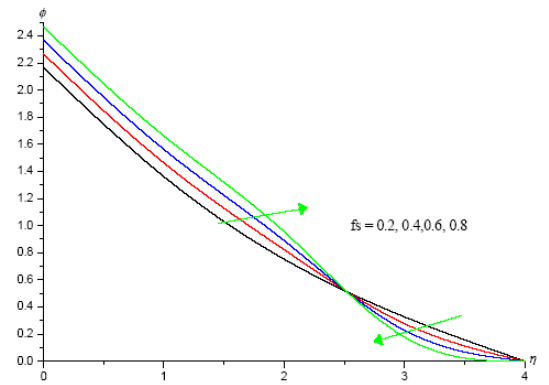


Fig.6d Variation of nanoconcentration(ϕ) with fs
 $m=0.5, R=0.5, Rd=0.5, Ec=0.01, A11=0.2, A22=-0.02$

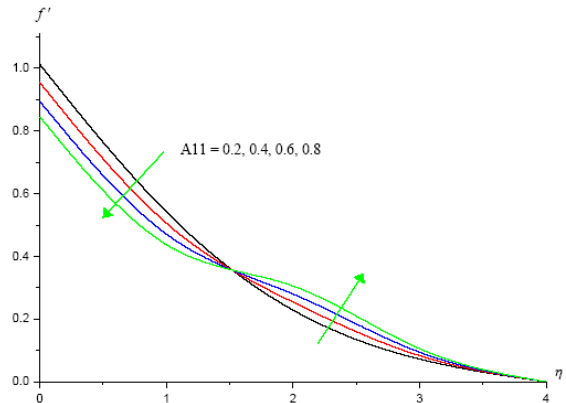


Fig.7a Variation of axial velocity(f') with $A11$
 $m=0.5, R=0.5, Rd=0.5, Ec=0.01, fs=0.2, A22=-0.02$

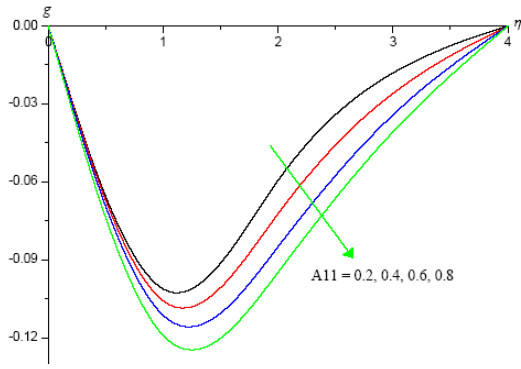


Fig. 7b Variation of secondary velocity(g) with A_{11}
 $m=0.5, R=0.5, Rd=0.5, Ec=0.01, fs=0.2, A_{22}=-0.02$

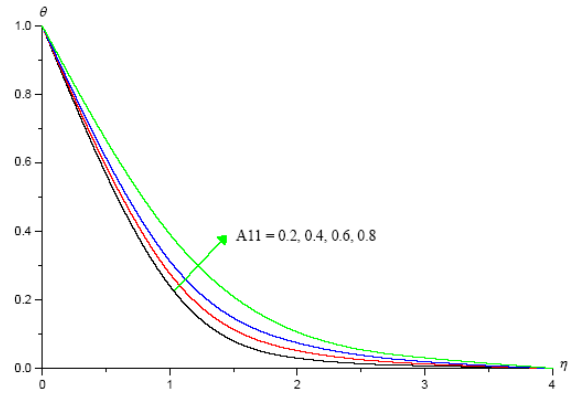


Fig. 7c Variation of temperature(θ) with A_{11}
 $m=0.5, R=0.5, Rd=0.5, Ec=0.01, fs=0.2, A_{22}=-0.02$

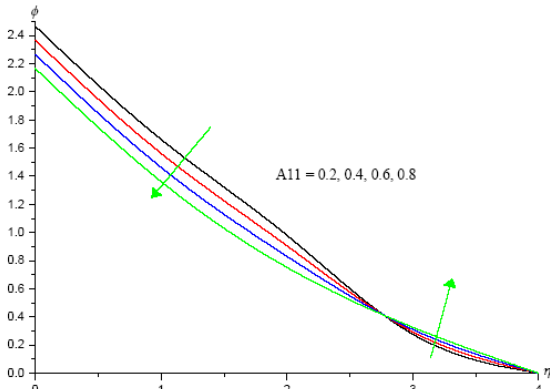


Fig. 7d Variation of nanoconcentration(ϕ) with A_{11}
 $m=0.5, R=0.5, Rd=0.5, Ec=0.01, fs=0.2, A_{22}=-0.02$

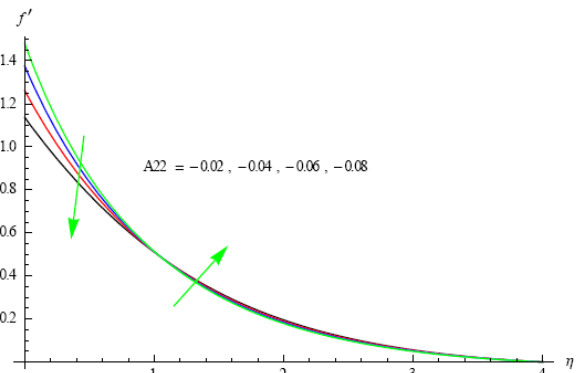


Fig. 8a Variation of axial velocity(f') with A_{22}
 $m=0.5, R=0.5, Rd=0.5, Ec=0.01, fs=0.2, A_{11}=0.2$

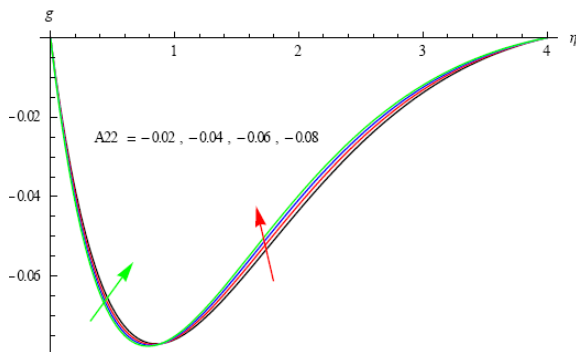


Fig. 8b Variation of secondary velocity(g) with A_{22}
 $m=0.5, R=0.5, Rd=0.5, Ec=0.01, fs=0.2, A_{11}=0.2$

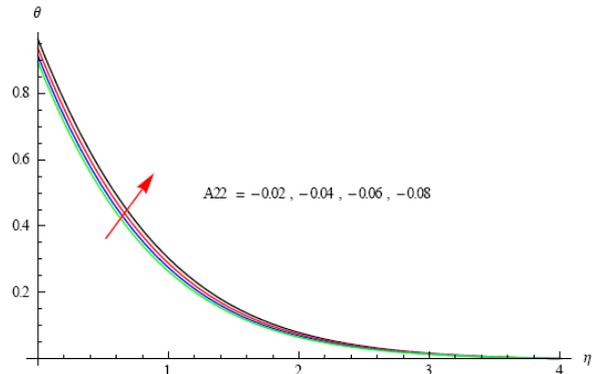


Fig. 8c Variation of temperature(θ) with A_{22}
 $m=0.5, R=0.5, Rd=0.5, Ec=0.01, fs=0.2, A_{11}=0.2$

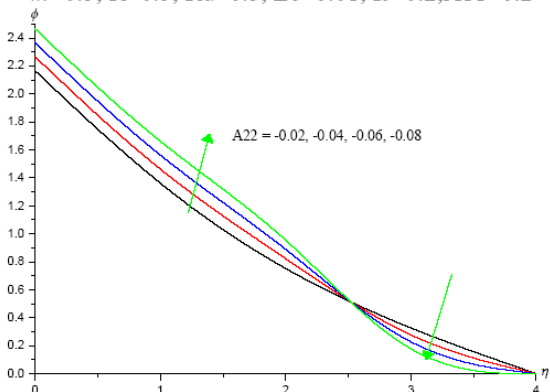


Fig. 8d Variation of nanoconcentration(ϕ) with A_{22}
 $m=0.5, R=0.5, Rd=0.5, Ec=0.01, fs=0.2, A_{11}=0.2$

Rotating MHD Heat and Mass Transfer Flow of Nanofluid past Exponentially Stretching Sheet with Second Order Slip

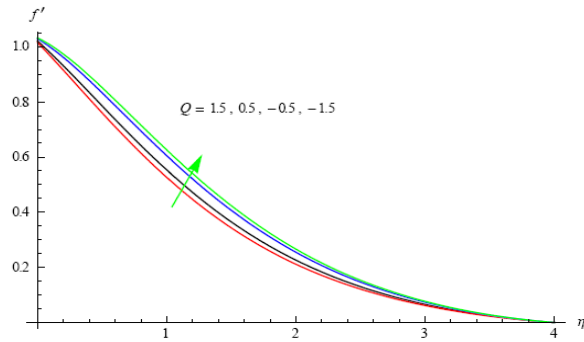


Fig.9a Variation of axial velocity(f') with Q
 $m=0.5, R=0.5, Rd=0.5, Ec=0.01, fs=0.2, A11=0.2$

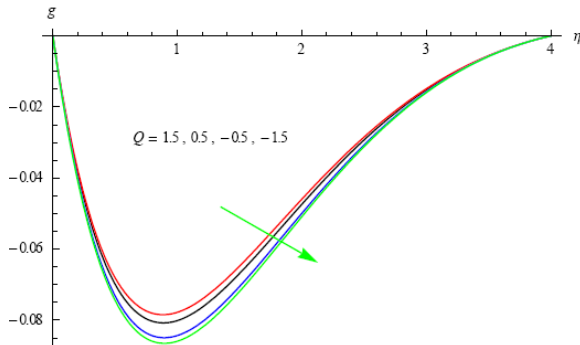


Fig.9b Variation of secondary velocity(g) with Q
 $m=0.5, R=0.5, Rd=0.5, Ec=0.01, fs=0.2, A11=0.2$

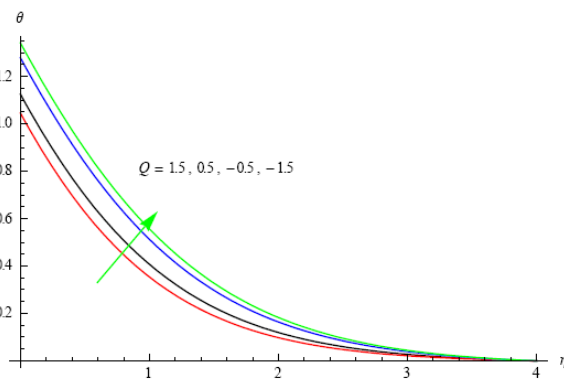


Fig.9c Variation of temperature(θ) with Q
 $m=0.5, R=0.5, Rd=0.5, Ec=0.01, fs=0.2, A11=0.2$

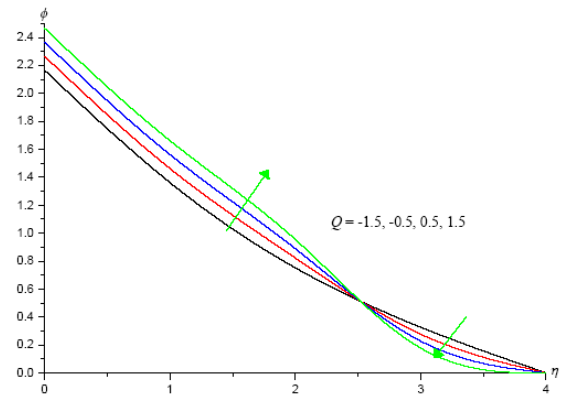


Fig.9d Variation of nanoconcentration(ϕ) with Q
 $m=0.5, R=0.5, Rd=0.5, Ec=0.01, fs=0.2, A11=0.2$

Table - 1 :

In the absence of convection ($G=0, N=0$), Chemical reaction ($\gamma=0$) the results are respectable agreement with *Bhim Sen Kala et al. [2]*

Parameters				Bhim Sen Kala et al. [2] Results				Present Results			
M	K_1	F_s	R	$f''(0)$	$g'(0)$	$-\theta'(0)$	$-\phi'(0)$	$f''(0)$	$g'(0)$	$-\theta'(0)$	$-\phi'(0)$
0.5	1	0.5	0.01	-0.7914	-0.0365	0.3885	1.9228	-0.7912	-0.0361	0.3881	1.9224
0.7	1	0.5	0.01	-0.6559	-0.0564	0.4532	1.9655	-0.6549	-0.0562	0.4528	1.9651
1.0	1	0.5	0.01	-0.4363	-0.0919	0.5113	2.0118	-0.4361	-0.0913	0.5109	2.0111
0.5	2	0.5	0.01	-0.6206	-0.6185	0.4646	1.9735	-0.6202	-0.6180	0.4638	1.9729
0.5	3	0.5	0.01	-0.7361	-0.0443	0.4211	1.9459	-0.7359	-0.0439	0.4207	1.9452
0.5	1	1.0	0.01	-0.5789	-0.0366	0.4351	1.9816	-0.5782	-0.0364	0.4346	1.9811
0.5	1	1.2	0.01	-0.4814	-0.0237	0.4536	2.0035	-0.4812	-0.0236	0.4527	2.0034
0.5	1	0.5	0.03	-0.8049	-0.1353	0.3526	1.9230	-0.8043	-0.1349	0.3523	1.9227
0.5	1	0.5	0.05	-0.8283	-0.2177	0.3103	1.9151	-0.8279	-0.2167	0.3101	1.9149

Table - 2

Skin Friction (τ_x), Nusslet number (Nu) and Sherwood Number (Sh) at $\eta = 0$

Parameter	$\tau_x(0)$	$\tau_z(0)$	Nu(0)	Sh(0)	Parameter	$\tau_x(0)$	$\tau_z(0)$	Nu(0)	Sh(0)		
m	0.5	-0.529239	-0.22973	1.00663	0.456234	fs	0.2	-0.529239	-0.22973	1.00663	0.456234
	0.75	-0.520672	-0.224759	1.0081	0.456145		0.4	-0.261377	-0.224275	0.99244	0.457818
	1	-0.50416	-0.229862	1.01086	0.455974		0.6	0.0402668	-0.21769	0.975052	0.459849
	1.5	-0.496562	-0.241692	1.01207	0.455895		0.8	0.455185	-0.207857	0.948654	0.463152
R	0.5	-0.529239	-0.22973	1.00663	0.456234	A11	0.2	-0.529239	-0.22973	1.00663	0.456234
	1	-0.545243	-0.357393	1.00314	0.45639		0.4	-0.396601	-0.224678	0.992507	0.457598
	1.5	-0.625571	-0.709933	0.984771	0.457215		0.6	-0.32321	-0.221837	0.984555	0.458386
	2	-0.768731	-1.08984	0.948668	0.458902		0.8	-0.27281	-0.219866	0.979036	0.458942
Rd	0.5	-0.529239	-0.22973	1.00663	0.456234	A22	-0.02	-0.825705	-0.240649	1.03709	0.453439
	1.5	-0.399928	-0.239792	0.885152	0.466427		-0.04	-1.13026	-0.251366	1.06683	0.450887
	3.5	-0.287215	-0.247928	0.802851	0.474888		-0.06	-1.41504	-0.260964	1.0933	0.448749
	5	-0.0966042	-0.260362	0.695807	0.488688		-0.08	-1.68238	-0.269631	1.11702	0.446931
Ec	0.01	-0.529239	-0.22973	1.00663	0.456234	Q	0.5	-0.416036	-0.237774	0.889192	0.468011
	0.03	-0.525935	-0.229977	1.00285	0.456551		1.5	-0.485362	-0.232917	0.957254	0.460816
	0.05	-0.522801	-0.230211	0.999291	0.456851		-0.5	-0.280977	-0.246605	0.782487	0.482095
	0.07	-0.51657	-0.230676	0.992316	0.457443		-1.5	-0.22513	-0.25002	0.745832	0.48802

2. Outcomes and Conversation

The non-dimensional direct speed $f'(\eta)$, rotational velocity $g(\eta)$, temperature $\theta(\eta)$ and nanoparticle capacity fraction $\phi(\eta)$ for different estimations of numerous boundaries are shown in figs.2-8.

Figs.2a-2d shows the assortment of f' , g , θ and ϕ with revolution boundary Hall parameter (m). It is discovered that an expansion in Hall boundary upgrades the straight and rotational speeds, nanoparticle volume portion and diminishes the temperature. This is because of the way that an expansion in the Hall boundary (m) expands the thickness of the direct and rotational limit layers and diminishes the thickness of the warm limit layer. Likewise the solutal limit layer thickness gets thicker for higher estimations of Hall boundary.

Figs. 3a-3d show the variety of f' , g , θ and ϕ with revolution boundary (R). We find that the straight and precise speed of the liquid increment with increment in revolution boundary R. On the other hand, the temperature increases and the nanoparticle volume partition decline with increase in R. Along these lines, speed limit thickness and exact speed limit layer thickness gets thicker, and as far as possible layer thickness gets thicker while the nanoparticle volume parcel limit layer thickness gets more thin for greater assessments of R.

The impact of dissemination (Ec) on f' , g , θ and ϕ is seen from figs.5a-5d. Higher the dissemination energy bigger the straight, precise speeds, temperature while more modest the nanoparticle volume division. Consequently, the thickness of the direct and rakish speed limit layer gets thicker with increment in Ec. The warm limit layer thickness gets thicker while that of nanoparticle volume portion gets more slender with higher estimations of Ec.

Figs.6a-6d show f' , g , θ and ϕ with Forchheimer boundary fs It tends to be seen from the profiles that the straight speed lessens in the stream district (0,1) and upgrades in the stream region(1,4)and rakish speed of the liquid increments with increment of Forchheimer boundary fs. The temperature improves while the nanoparticle volume portion decreases with increment in fs. Thus, the thickness of the straight and precise speed limit layers become thicker. The thickness of the warm limit layer gets thicker while the thickness of the nanoparticle volume portion limit layer gets more slender for enormous estimations of fs.

Figs.7a-7d speak to the variety of f' , g , θ and ϕ with first request slip boundary (A11). The straight and rotational speeds diminish in the stream area (0, 1) while in the excess district (1, 4) the direct speed decreases and the rotational speed improves with increase in A11. The temperature improves and nanoparticle volume division decreases with A11. This is because of the way that an expansion in A11 lessens the thickness of the force, nanoparticle volume part while the warm limit layer gets thicker.

Figs.8a-8d portrays the variety of f' , g , θ and ϕ with second request slip boundary (A22). The direct and rotational speeds upgrade in the district (0, 1) and lessen in the area (1, 4). The temperature decreases and the nanoparticle volume division improves with increment in A22. In this way the thickness of the warm limit layer gets more slender and that of nanoparticle volume portion gets thicker.

Fig. 9a-9d display f' , g , θ and ϕ with variety in heat source boundary Q. It tends to be seen from the profiles that within the sight of warmth source the direct and rotational speeds, temperature diminishes while nanoparticle volume part increments and a turned around impact is seen within the sight of warmth assimilation. The is because of the way that an expansion in the liquid temperature causes more actuated stream towards the

Rotating MHD Heat and Mass Transfer Flow of Nanofluid past Exponentially Stretching Sheet with Second Order Slip

plate through the warm lightness impact and subsequently the thickness of the warm limit layer is decreasing for higher estimation of Q .

We, by and by analyze the assortments of the genuine measures of planning hugeness, that is the close by skin scouring coefficient for direct speed, C_f , neighborhood skin disintegration coefficient for rotational speed C_g and the close by Nusselt number Nu , neighborhood Sherwood number for different assessments of m , R , Q , Ec , fs , $A11$ and $A22$. The amounts $f''(0)$, $g'(0)$, $\theta'(0)$ and $\phi'(0)$ related to close by skin grinding coefficient for straight speed (C_f), neighborhood skin contact coefficient for rotational speed (C_g), the close by Nusselt Number (Nu), neighborhood Sherwood number (Sh) are given in table.2 for various assessments of limits.

From Table 2 it is observed that the skin friction f'' and g' reduces with increase in $m \leq 0.75$ and for higher $m \geq 1.0$, f'' reduces and g' enhances with m at the wall. The porous parameter enhances f'' and reduces g' on the wall. The rate of heat transfer enhances and rate of mass transfer reduces at the wall with increase in porous parameter. Higher the rotation parameter (R) larger the f'' and g' at the wall, Nusselt number Nu reduces and Sherwood number Sh enhances at $\eta=0$. In the presence of heat generating / absorbing source f'' increases and g' decreases at the wall. Higher Radiation heat flux (Rd) / Dissipation (Ec) decreases (C_f), (Nu), enhances (C_g) and (Sh) on $\eta=0$. The Nusselt number increases and Sherwood number decreases with increase in $Q > 0$ while a reversed effect is noticed in their behaviour with increase in $Q < 0$. An increase in Forchheimer parameter (fs) reduces the skin friction coefficients, Nu and enhances the rate of mass transfer at the wall. τ_x, τ_z , Nu enhance, Sh reduces with increase in first order parameter ($A11$) while an increase in second order parameter ($A22$) increases τ_x, τ_z , Nu and reduces, Sh at the wall $\eta=0$.

3. Conclusions

- From this examination we locate that an expanding corridor boundary (m) builds speed part, temperature and focus.
- Higher the Turn boundary (R) little the hub speed, bigger auxiliary speed, temperature and focus.
- Higher the Radiation boundary (Rd)/Eckert number (Ec) builds a speed part, temperature and lessens focus.
- An expanding Forchheimer boundary (fs) least to an upgrade a speed, temperature and focus.
- An increment in second request slip ($A22$) diminishes a speed part in the locale (0, 1) and improves in the district (1, 4). The temperature encounters an upgrade in the whole stream district. The Nano-focus improves in the locale (0, 2.5) and lessens in the area (2.5, 4).

Acknowledgements

I would also like to thank who helped me a lot in finalizing this project within the limited time frame. .

References

- [1] Ariel, P.D. (2007). Asymmetric flow due to a stretching sheet with partial slip, *Compt. Math. Appl.* Vol.54, pp.1169–1183.
- [2] Bhim Sen Kala, Rawat, M.S. and Komal. (2015). Effect of magnetic, permeability and Forchheimer parameters on steady MHD flow of nanofluids with rotation through non-darcy porous medium over exponentially stretching porous sheet, *Int. J. of Math. Archive*, Vol.6 (9), pp.133-146.
- [3] Choi, C.H., Westin J.A. and Breuer K.S. (2002). To slip or not to slip water flows in hydrophilic and hydrophobic micro channels. *Proceedings of IMECE 2002*, New Orleans, LA, Paper No.2002-33707
- [4] Das, K. (2012). Slip flow and convective heat transfer of nanofluids over a permeable stretching surface, *Comput. Fluids*, Vol.64, pp.34–42.
- [5] Kalidas Das, Amit Sarkar and Prabir Kumar Kundu. (2017). Cu-water Nanofluid flow induced by a vertical stretching sheet in presence of a magnetic field with convective heat transfer, *Propulsion and Power Research*, Vol. 6(3), pp.206-213. <http://dx.doi.org/10.1016/j.jprr.2017.07.001>.
- [6] Mabood, F. and Khan W.A. (2014). Approximate analytic solutions for influence of heat transfer on MHD stagnation point flow in porous medium, *Comput. Fluids*, Vol.100, pp.72–78.
- [7] Martin, M.J. and Boyd I.D. and Blasius. (2000). Boundary layer solution with slip flow conditions, in: *Proceedings of the 22nd Rarefied Gas Dynamics Symposium*, Sydney, Australia.

- [8] Martin, M.J. and Boyd I.D. (2006). Momentum and heat transfer in a laminar boundary layer with slip flow, *J. Thermophys. Heat. Transf.*, Vol.20(4), pp.710–719.
- [9] Matthews, M.T. and Hill J.M. (2007). Nano boundary layer equation with nonlinear Navier boundary condition, *J. Math. Anal. Appl.*, Vol.333, pp.381–400.
- [10] Navier, C.L.M.H. (1823). Mémoire sur les lois du mouvement desfluids, *Mém. Acad. R. Sci. Inst. Fr.*, Vol.6, pp.389–440.
- [11] Pavitra, G.M and Gireesha, B.J (2013). Unsteady flow and heat transfer of a fluid particle suspension over an exponentially stretching sheet ,*Journal of Heat transfer*, Vol.5, pp.613-624.
- [12] Sandeep, N., Sulochana, C. and Rushi Kumar. B. (2016). Unsteady MHD radiative flow and heat transfer of a dusty Nanofluid over an exponentially stretching surface, *Engineering Science and technology, an international Journal*, Vol.19, pp.227-240.
- [13] Sandeep, N., Sulochana, C., Raju, C.S.K., Jayachandra babu, M. and Sugunamma, V. (2015). Unsteady boundary layer flow of thermophoretic MHD Nanofluid past a stretching sheet with space and time dependent internal heat source/sink, *Applications and Applied Mathematics, an International Journal*, Vol.10(1), pp.312-327.
- [14] Sarojamma, G., Syed Mahaboobjan and Nagendramma,V. (2015). Influence of Hall currents on cross diffusive convection in a MHD boundary layer flow on stretching sheet in porous medium with heat generation., *International Journal of Mathematical Archieve*, Vol.6(3), pp.227-248.
- [15] Sarojamma, G, Syed Mahaboobjan and Sreelakshmi, K. (2015). Effect of Hall current on the flow induced by a stretching surface., *International journal of Scientific and Innovative Mathematical Research*,Vol.3(3), pp.1139-1148
- [16] Shikhmurzaev, Y.D. (1993). The moving contact line on a smooth solid surface, *Int. J. Multiph. Flow*, Vol.19, pp.589–610.
- [17] Sugunamma, V, Sandeep, N and Sulochana, C. (2015). MHD boundary layer flow past an exponentially stretching sheet, *International Journal of Science and Innovative Mathematical Research*, Vol.3(3), pp.902-906.
- [18] Swathi Mukhopadyay. (2013). MHD boundary layer flow and heat transfer over an exponentially stretching sheet embedded in a thermally stratified medium, *Alexandria Engineering Journal*, Vol.52, pp.2659-265.
- [19] Wang, C.Y. (2009). Analysis of viscous flow due to a stretching sheet with surface slip and suction, *Nonlinear Anal. Real. World Appl.*, Vol.10, pp.375–380.
- [20] Wang, X.Q and Mazumdar, A.S. (2007). Heat transfer characteristics of nanofluids, a review, *Int. J. Thermal Sci.*, Vol.46, pp.1-19.
- [21] Zaimi, K and Pop, I. (2014). Flow past a permeable stretching / shrinking sheet in a Nanofluid using two phase model, *Plops one.*, Vol.9(11), p.e111743